The Journal of Experimental Biology 200, 161–171 (1997)
Printed in Great Britain © The Company of Biologists Limited 1997
JEB0629

DYNAMIC IMAGING OF FUNCTIONAL NERVE TERMINALS AND SCHWANN CELLS IN PRESYNAPTIC 'NERVE PLATES' ISOLATED FROM THE SKATE ELECTRIC ORGAN

MICHAEL J. DOWDALL*, A. CHRIS GREEN* AND C. MARK RICHARDSON†
Department of Life Science, University of Nottingham, Nottingham NG7 2RD, UK

Accepted 21 October 1996

Summary

The cholinergic innervation and its glial support were isolated in a functional state from the electric organ of the skate (*Raja* species) using a combined enzymatic and mechanical dissociation technique. Examination using light and electron microscopy showed that this 'nerve plate' is a disc-shaped structure several hundred micrometres in diameter consisting of a dense plexus of nerve terminals attached to branching nerve fibrils with numerous associated myelinating and perisynaptic Schwann cells. In unfixed nerve plates, depolarisation and Ca^{2+}-dependent staining of the nerve terminals was seen with RH-414, a fluorescent marker for functional motor terminals. The components of the nerve plate could be loaded with the Ca^{2+}-sensitive dyes Fluo-3 and Fura-2. Depolarisation of nerve plates loaded with either dye leads to an immediate increase of intracellular Ca^{2+} levels ($[Ca^{2+}]_i$) in the nerve terminals. This response was blocked by certain Ca^{2+} channel antagonists from the ω-conotoxin family. Glial cell responses to depolarisation were in general minimal. However, increases of $[Ca^{2+}]_i$ were seen in these cells, but not in nerve terminals, during applications of ATP and acetylcholine. These results show that both nerve terminal and glial elements in this 'nerve plate' preparation are functional. The ease of this preparation and its functional reliability give it considerable potential as a useful model for elucidating presynaptic mechanisms.

Key words: skate, electric organ, nerve terminals, Schwann cells, presynaptic Ca^{2+} channels, purinoceptors, *Raja* spp.

Introduction

Skate (*Raja* spp.) are weakly electric marine rays (Bennett, 1961, 1970) which generate small discharges of 1–4 V from paired, spindle-shaped electric organs located amongst the tail musculature. They are situated in the position normally occupied by the lateral muscle bundle and extend along most of the length of the tail almost to its tip (Ewart, 1888; Sanderson and Gotch, 1888, 1889). Each organ consists of thousands of polygonal capsules (termed 'electroplates' by Brock *et al.* 1953) longitudinally organised into loose columns of several hundred electroplates in series. The anterior section of each capsule is occupied by a single electrocyte densely innervated on its anterior surface. The skate electric organ, like that in *Torpedo* spp., is closely related to vertebrate skeletal muscle in its embryological origin (Couteaux, 1963; Ewart, 1892) and its cholinergic innervation (Brock *et al.* 1953).

Measurements of biochemical markers for cholinergic nerve terminals show that the synaptic density in skate electric organ is much greater than that in skeletal muscle but somewhat less than that in *Torpedo* spp. (Dowdall *et al.* 1989; Kriebel *et al.* 1996). Although not ideally suited to conventional biochemical investigations of synaptic mechanisms because of its small size, the skate electric organ has several useful features encouraging such studies. With *Torpedo* electric organ, the isolation and purification of cellular and subcellular structures requires an initial disruption of the tissue using harsh mechanical methods (Dowdall and Zimmerman, 1977). With skate, but not *Torpedo*, collagenase treatment leads to complete dissociation of the organ, producing intact functional electrocytes (Fox *et al.* 1990). Initially, these electrocytes are fully innervated, but sustained collagenase treatment eventually results in complete denervation of otherwise intact electrocytes (Fox *et al.* 1990; Kriebel *et al.* 1996). During collagenase denervation, some nerve terminals become completely detached from all associated cellular elements (Dowdall *et al.* 1989; Kriebel *et al.* 1996) whilst others remain with the matrix-like sheet of presynaptic material (see 'nerve ending clusters' in Kriebel *et al.* 1996). In these earlier studies, attention was focused on isolating detached nerve terminals. This proved to be technically difficult owing to their fragility and low yield (Kriebel *et al.* 1996). Here, we have therefore taken an alternative approach and investigated some properties of the nerve terminals which remain associated with the presynaptic plexus.

In this report, we describe the preparation, morphology and

*Authors for correspondence [e-mail (A.C.G.): plzacg@pln1.life.nottingham.ac.uk].
†Present address: Department of Anatomy, School of Medical Sciences, University of Bristol, Bristol BS8 1TD, UK.

functional properties of the multicellular presynaptic plexus which constitutes the innervation apparatus of the electrocyte. These structures, which we call 'nerve plates', can be readily isolated in small numbers from the collagenase-digested electric organ. We have used optical imaging technology to study the dynamic functional properties of the nerve terminals and Schwann cells in the nerve plate complex. Evidence is provided that nerve terminals have resting potentials and, when depolarised, release transmitter by a Ca^{2+}-dependent process and also undergo membrane recycling. In addition, it is shown that the Schwann cells in the complex show Ca^{2+} mobilisation responses to some extracellularly applied chemical mediators. It is suggested that the nerve plate preparation is a useful additional model for studying presynaptic physiology and biochemistry.

Materials and methods

Collagenase (type A) and dispase (grade II) were obtained from Boehringer Mannheim (Germany). The Ca^{2+}-sensitive probes Fluo-3AM, Fura-2AM and Fura-2 pentasodium salt were from Calbiochem (USA) and RH-414 was obtained from Molecular Probes (USA). The Ca^{2+} channel antagonists ω-conotoxins GVIA, MVIIA and MVIIC were from Bachem (USA), whilst ω-conotoxin SVIB and ω-agatoxin IVA were from the Peptide Institute (Japan). Other chemicals and drugs were from a variety of sources and were of the best grade available. Skate were collected from the Marine Biological Association Laboratory at Plymouth and were maintained in tanks of recirculating sea water at 13 °C under a 12 h:12 h light:dark cycle until required. Three species were used in this study: *Raja clavata* L., *R. montagui* Fowler and *R. brachyura* Lafont. Fish were killed and electric organs dissected from the tail essentially as described previously (Kriebel *et al.* 1996; Richardson *et al.* 1995). Organs were placed in small plastic Petri dishes and covered with skate Ringer (SR) of the following composition (in mmol l^{-1}): NaCl, 280; KCl, 6; $CaCl_2$, 4.4; $MgCl_2$, 1.8; urea, 360; glucose, 1; and Hepes buffer, 10; pH 7.3. Organs and their sections were stored in a refrigerator at 4 °C until required (up to 5 days).

Isolation of innervated electrocytes

Innervated electrocytes were prepared after collagenase treatment of electric organs which had been sectioned into lengths of approximately 5 mm. The initial phase of this exposure to collagenase (7.5 mg ml^{-1}) was an overnight (16–18 h) incubation of tissue at 4 °C. This was followed by a transfer to room temperature (approximately 25 °C) for 2–3 h. The state of tissue dissociation was assessed by inspection under a binocular dissecting microscope, and incubation was terminated by the addition of ice-cold SR, supplemented with bovine serum albumin (BSA, 1 mg ml^{-1}), and gentle dispersion of the cellular mass using a plastic Pasteur pipette. The appropriate 'end point' could be recognized with experience gained during successive trials. If the incubation period at room temperature was too short, the tissue did not fully dissociate and only limited numbers of individual electrocytes were obtained. Following prolonged incubation, nerve plates became detached from electrocytes before or during tissue dispersion. Innervated electrocytes were collected from dispersed tissue by repeated (4–5) sedimentations at 1 ***g*** in ice-cold SR with added BSA. The addition of BSA to the SR markedly reduced the tendency of the electrocytes to adhere to the surfaces of the containers and transfer pipettes used during electrocyte isolation. This procedure removed small cellular debris along with the collagenase. Washed electrocytes were maintained in this medium at 4 °C until required. In a typical isolation using 100–300 mg of electric organ, several hundred electrocytes were produced.

Separation of nerve plates from innervated electrocytes

Electrocytes were washed twice in BSA-free SR and then transferred to a glass coverslip (22 mm×22 mm) in a droplet of fluid (10–20 cells). Free-floating electrocytes were viewed under a binocular dissection microscope and allowed to settle plate-side down, this being encouraged where necessary by gentle manipulation using a fine probe. After allowing a few minutes for nerve plates to establish a firm bonding to the coverslip, their attached, overlying electrocytes were removed using fine forceps. This procedure involved gripping the electrocyte at its lateral extremity and gently peeling it away from the adherent nerve plate. Fluid containing these detached electrocytes was removed from the coverslip and replaced with fresh SR. Coverslips with attached nerve plates bathed in SR were stored at 4 °C until required (3–4 h).

Morphological techniques

Enzyme histochemical staining of acetylcholinesterase in cryostat sections of whole organ was carried out using acetylthiocholine as a substrate in the presence of ferricyanide and Cu^{3+}, as described by Karnovsky and Roots (1964). This method produced fine deposits of copper(III) ferrocyanide (Hatchett's Brown).

Samples for transmission electron microscopy were fixed for 2 h at room temperature with 2.5 % glutaraldehyde in 0.2 mol l^{-1} phosphate buffer (pH 7.4) containing 10 % sucrose. Fixative was removed and, after washing (three times) in the same buffer, samples were broken into fragments of approximately 1 mm^3. They were post-fixed with 1 % OsO_4 in 0.4 mol l^{-1} sodium phosphate buffer for 1 h, washed with water and then stained for 15 min with 1 % uranyl acetate in 0.25 mol l^{-1} sodium acetate buffer, pH 6.5. After ethanol dehydration, specimens were impregnated with 'Spurr' resin. Sections from polymerised resin blocks were counterstained with lead citrate before viewing in a Joel-100S transmission electron microscope. Sample preparation for scanning electron microscopy was essentially the same as described above for the fixation and dehydration stages except that the samples were attached to glass coverslips. After dehydration and critical-point drying, they were sputter-coated with gold and viewed under a Joel JSM-840 scanning electron microscope.

Dynamic imaging by fluorescence microscopy

For experiments using the Ca^{2+}-sensitive dyes Fluo-3 and

Fura-2, cell loading was carried out before mounting nerve plates in the perfusion/recording chamber. Coverslips were incubated for 45–60 min at room temperature (22–25 °C) with precursor esters (5 μmol l^{-1} Fluo-3 acetoxymethyl ester or 5 μmol l^{-1} Fura-2 acetoxymethyl ester) in SR containing 0.1 % BSA and 0.5 % dimethyl sulphoxide (dye solvent). Cover slips with dye-loaded nerve plates were placed in an enclosed perfusion/recording chamber (200 μl bath volume) and continuously perfused at 1.5–2 ml min^{-1} with SR. Perfusion was allowed to continue for at least 10 min prior to measurements being made to allow for complete de-esterification of the intracellular dye. To depolarise nerve plates, a modified SR (KSR) containing 80 mmol l^{-1} KCl and 208 mmol l^{-1} NaCl was used. Drugs and KSR were applied by bath perfusion with an exchange time of 5–7 s. All imaging experiments were conducted at room temperature.

The dye-loaded nerve plates were monitored optically using a Zeiss Axiovert 135 TV microscope equipped with epifluorescence and differential interference optics [40×, numerical aperture (NA) 1.3; 100×, NA 1.32; oil-immersion objectives]. Fluorescence from Fluo-3-loaded nerve plates (excitation 490 nm ± half band width of 7 nm; >515 nm emission) was imaged with an extended ISIS camera (Photonic Science) and the average of 8–10 video frames was captured every 2–12 s to the hard disc of an Apple Quadra 950 computer using IonVision software (Image Processing and Vision Company Ltd). Fluorescence intensity from areas corresponding to nerve terminals was determined after background subtraction (emission from a cell-free area of the coverslip), and the ratio of the fluorescence intensity (F) to the initial baseline fluorescence (F_0) was calculated. With Fura-2-loaded preparations, pairs of images (excitation at 340 and 380 nm ± half band widths of 6 nm; 500–530 nm emission) were captured every 2–12 s as described above. After background subtraction, ratios were calculated from the fluorescence intensities of the image pairs (340 nm/380 nm), and ratios from regions corresponding to nerve terminals and Schwann cells were converted to Ca^{2+} concentrations using the following equation:

$$[Ca^{2+}]_i = K_d(R - R_{min})/(R_{max} - R),$$

where K_d is the apparent dissociation constant, R is the fluorescence ratio, R_{min} is the fluorescence ratio in absence of Ca^{2+} and R_{max} is the fluorescence ratio at saturating Ca^{2+}. The values for K_d, R_{min} and R_{max} were determined by imaging the free acid of Fura-2 in a series of EGTA-buffered Ca^{2+} solutions (Molecular Probes) and were found to be 1686 nmol l^{-1}, 0.53 and 11.24, respectively.

When RH-414 was used to stain nerve terminals, it was added to the perfusion medium at 5 μmol l^{-1} for 2 min.

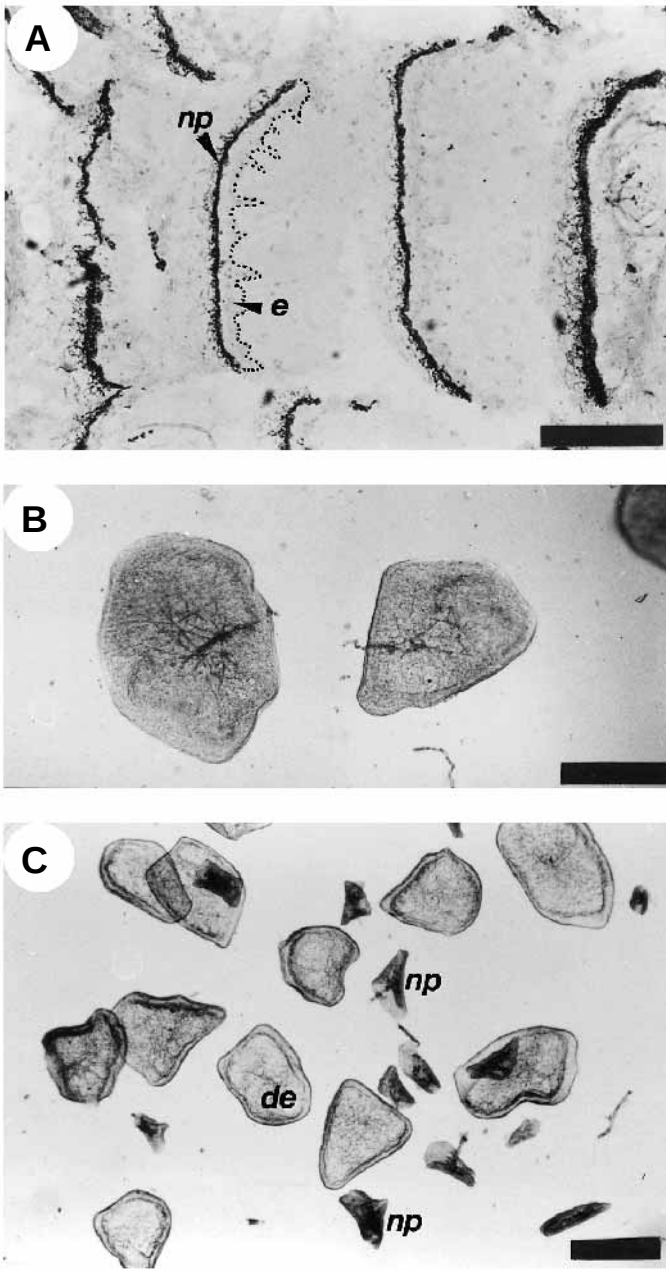

Fig. 1. Light micrographs of nerve plates *in situ* and in preparations of dissociated electrocytes isolated from *Raja clavata* electric organ. (A) The appearance of nerve plates in longitudinal cryostat sections of electric organ stained for acetylcholinesterase. The micrograph shows the innervation to a number of adjacent electrocytes by branching nerve fibrils which form dense networks at the anterior surface of each electrocyte. The electrocytes (*e*) are poorly stained in this enzyme histochemical procedure but are located to the right of the most intensely stained regions of each nerve plate (*np*). They have a convoluted non-innervated surface (that belonging to the labelled electrocyte has been outlined for clarity) and are between 20 and 30 μm thick. Scale bar, 250 μm. (B) Innervated electrocytes isolated by collagenase dissociation of the electric organ as described in Materials and methods. The branching nerve fibrils can be seen clearly on the surface of the electrocytes. Scale bar, 500 μm. (C) A mixture of nerve plates (*np*) and denervated electrocytes (*de*) prepared by inclusion of dispase (5 mg ml^{-1}) in the collagenase incubation medium. Scale bar, 500 μm. Similar preparations can be obtained by prolonged incubation in collagenase alone. Such preparations are not suitable for the isolation of immobilised nerve plates but provide a source of nerve plates more amenable to processing for transmission electron microscopy (see Fig. 3).

Manipulations of this loading medium were made as described in the text. Differential interference contrast and fluorescence (380–490 nm excitation; >515 nm emission) images were captured to computer hard disc *via* an integrating cooled CCD camera (Hamamatsu Colour Chilled CCD C5310) using MediaGrabber software (Raster Ops). Images were captured before, during and 10 min after RH-414 loading.

Results

The appearance of nerve plates *in situ* and in preparations of dissociated electrocytes is shown in Fig. 1. In tissue sections, the dense innervation is particularly evident after enzyme histochemical staining for acetylcholinesterase (Fig. 1A). Electrocytes isolated from collagenase-treated electric organ retain this 'plate' of innervation (Fig. 1B). Following prolonged incubation in collagenase (>96 h at 4 °C) or incubation in collagenase plus dispase (5 mg ml^{-1}), the nerve plates became detached from the electrocytes and could be recognised as separate structures in the suspension of cellular components collected after tissue dispersal (Fig. 1C).

Separation of nerve plates from innervated electrocytes

Collagenase-dissociated innervated electrocytes were found to be very 'sticky' structures which adhered strongly to glass and plastic surfaces during manipulations. We exploited the tight physical bonding between nerve plates and glass coverslips, which was of sufficient strength to permit the removal of electrocytes from the immobilised nerve plates. The morphological appearance of nerve plates at this stage of isolation

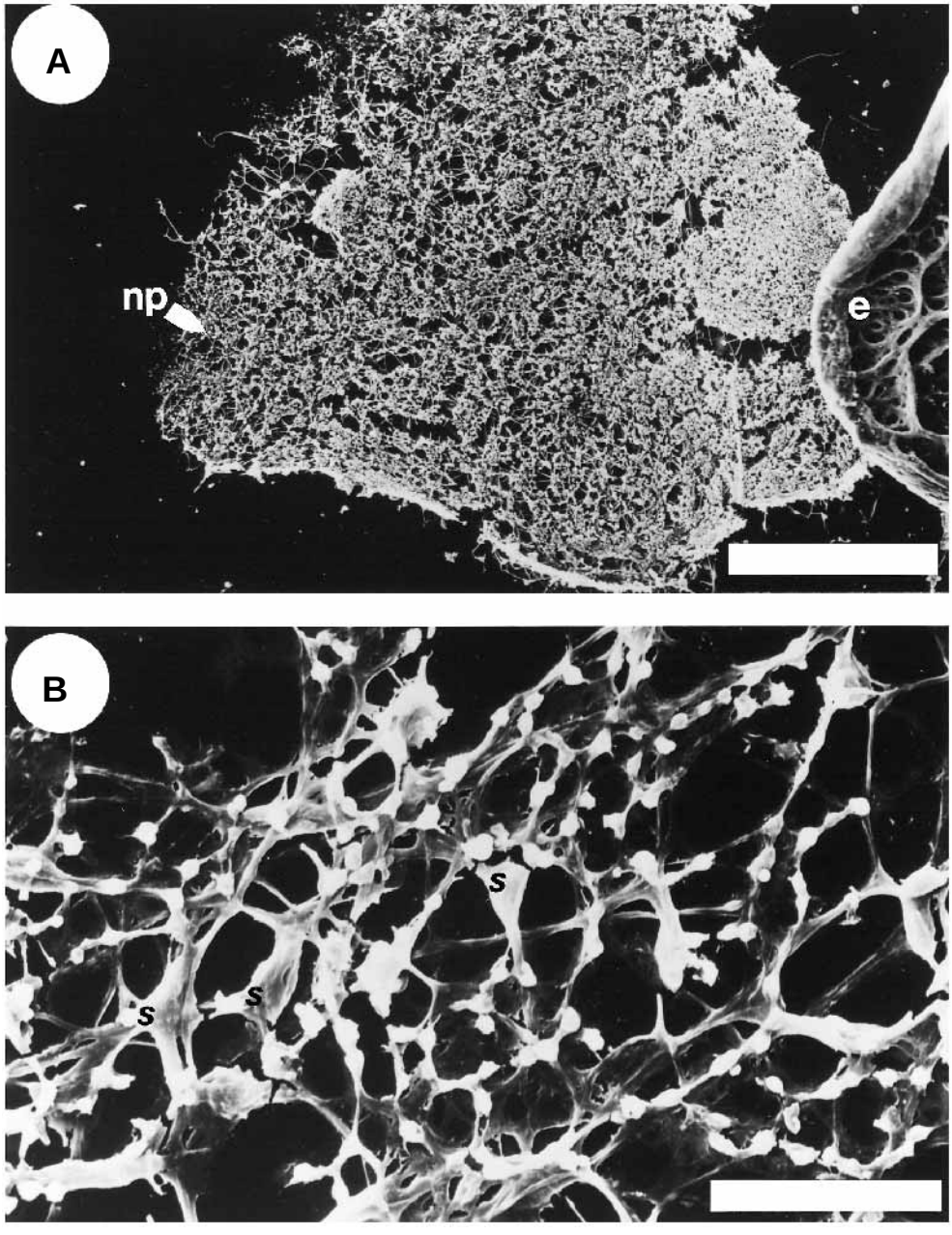

Fig. 2. Nerve plate structure revealed by scanning electron microscopy. Innervated electrocytes from *Raja montagui* electric organ were attached to glass coverslips, fixed and prepared for microscopy as described in Materials and methods. (A) Low-magnification view of the nerve plate (np) preparation. Part of the non-innervated surface of an electrocyte (e) can also be seen. Scale bar, 250 μm. (B) A detached nerve plate viewed at high magnification shows the arrangement of small round nerve terminals in a matrix of nerve fibrils and pyramid-shaped Schwann cell bodies (*s*). Scale bar, 25 μm.

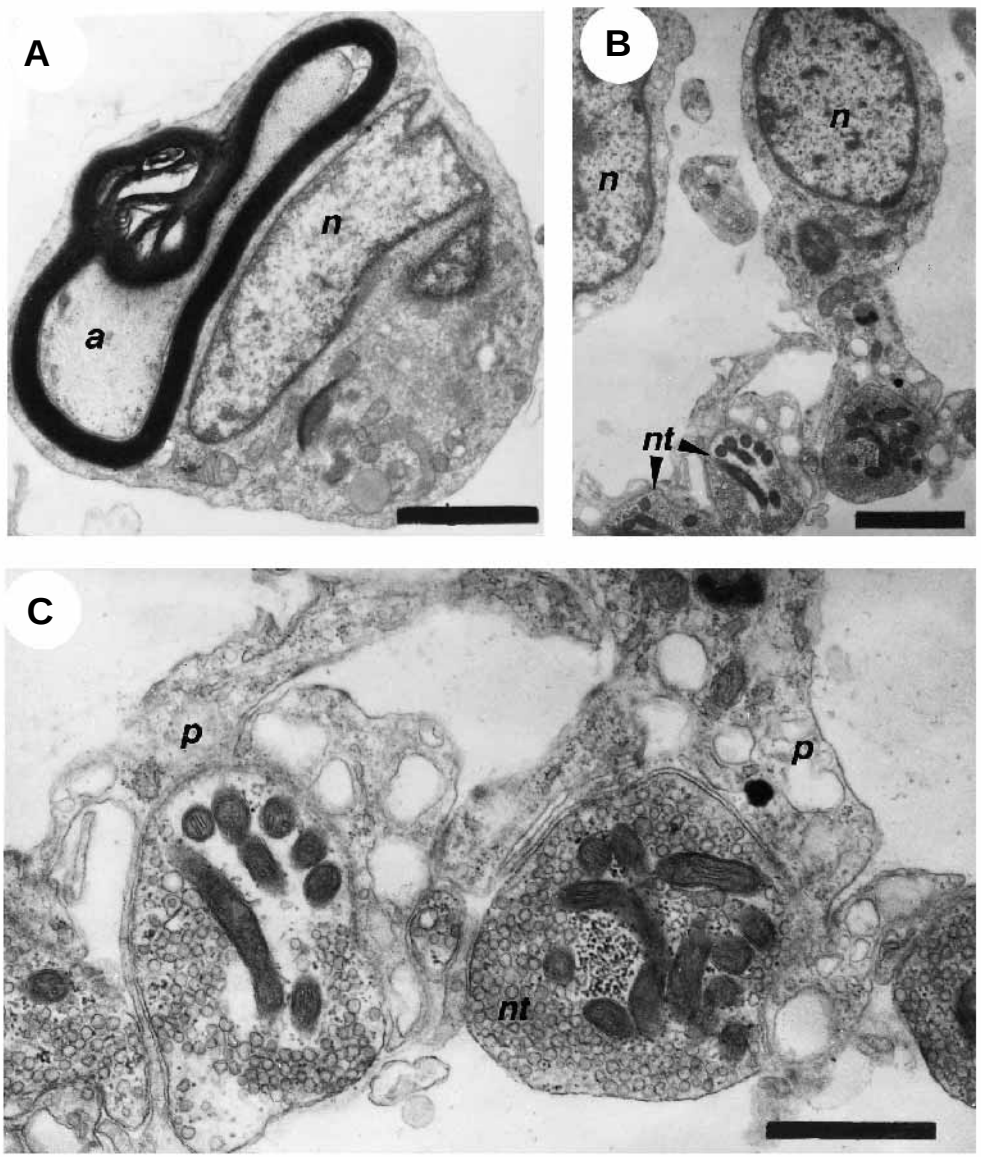

Fig. 3. Appearance of nerve terminals in nerve plates revealed by transmission electron microscopy. Nerve plates were collected from collagenase/dispase-treated electric organ (see Materials amd methods and Fig. 1) from *Raja montagui* and, after fixing, processed for microscopy as described in Materials and methods. (A) A section through a typical myelinating Schwann cell and nerve fibril (*a*). The nucleus (*n*) and myelin membranes are clearly visible. Such cells were restricted to localised regions of the nerve plate sections and were often found with numerous other myelinated nerve fibrils. Scale bar, 2 μm. (B) The majority of the nerve plate sections were made up of numerous non-myelinating Schwann cells (nuclei labelled *n*) interspersed with a large number of nerve terminals (*nt*). Scale bar, 2 μm. (C) Higher magnification of the nerve terminal region in B showing the intimate association between the nerve terminals (*nt*) and the perisynaptic Schwann cell processes (*p*). Nerve terminals can be seen to possess numerous synaptic vesicles, glycogen granules and intraterminal mitochondria. Scale bar, 1 μm.

can be seen in Fig. 2. At low magnifications, the immobilised nerve plate and the convoluted non-innervated face of the electrocyte are clearly visible (Fig. 2A). Higher magnification shows the arrangement of the small round terminals embedded in a matrix of branching nerve fibrils and pyramid-shaped Schwann cells (Fig. 2B). A feature of these micrographs from scanning electron microscopy was the smaller apparent size of the nerve terminals and Schwann cells than was seen with transmission electron microscopy and in unfixed preparations viewed by differential contrast light microscopy (see below and Fig. 4). This ‘shrinkage’ may be due to the fixation and/or processing techniques used for scanning electron microscopy.

Further detail of the ultrastructure of the cellular elements in the nerve plate plexus can be seen in the transmission electron micrographs (Fig. 3). Myelinated nerve fibrils and myelinating Schwann cells (Fig. 3A) formed a minor part of the nerve plate. A greater contribution was made by the large numbers of nerve terminals intermixed and closely associated with non-myelinating, perisynaptic Schwann cells (Fig. 3B,C). The latter had extensive fine processes which were often seen encapsulating individual nerve terminals (Fig. 3C). The morphology of the nerve terminals with synaptic vesicles, mitochondria and electron-dense glycogen granules was essentially the same as reported previously for other skate species (Fox *et al.* 1990; Kriebel *et al.* 1996).

Staining of nerve terminals with RH-414

The fluorescent dye RH-414 is a useful dynamic stain for functional motor nerve terminals (Betz *et al.* 1992). It becomes incorporated into synaptic vesicle membranes at active terminals following transmitter release and subsequent membrane recycling. In isolated nerve plates loaded with RH-414 in SR and subsequently washed for 10 min, little or no staining was seen in any structures. If loading was carried out under depolarising conditions which cause transmitter release (i.e. in KSR; see Richardson *et al.* 1995, 1996), RH-414 fluorescence was located

exclusively in the nerve terminals (Fig. 4). No staining of the Schwann cells or nerve fibrils was seen. No staining was seen if RH-414 loading took place in SR or if transmitter release was prevented by the presence of the Ca^{2+} channel antagonist ω-conotoxin MVIIC (1 μmol l^{-1}; Richardson *et al.* 1995, and see below) before and during the K^+ depolarisation. Thus, our results with RH-414 suggest that the nerve terminals in the nerve plate preparation are functionally intact.

Nerve terminals and Ca^{2+} responses

The Ca^{2+}-sensitive fluorescent dyes Fluo-3 and Fura-2 were used to follow changes in intracellular Ca^{2+} concentration triggered by depolarisation of nerve plates with KSR. Satisfactory loading of the nerve terminals with these dyes was achieved after a 45–60 min of incubation with their precursor acetoxymethyl esters. Using the ratiometric dye Fura-2, calibration of the fluorescence signals showed that, in resting nerve terminals, $[Ca^{2+}]_i$ was in the range 10–40 nmol l^{-1} (see Figs 6, 7). Upon depolarisation with KSR, there was an immediate and dramatic increase in intracellular Ca^{2+} concentration with peak values in the range 300–1000 nmol l^{-1} (see Fig. 6). This response was typically biphasic with a sustained plateau phase following an initial peak response (Fig. 5). When depolarised nerve plates were returned to SR, the elevated $[Ca^{2+}]_i$ rapidly declined to baseline values. When nerve plates were depolarised in nominally Ca^{2+}-free KSR, the nerve terminal response was reduced by 95 %. Thus, the rise in intracellular Ca^{2+} concentrations depended on the presence of extracellular Ca^{2+} and was probably mediated by Ca^{2+} entry *via* voltage-sensitive presynaptic Ca^{2+} channels (Fig. 5A). In nerve plates subjected to repeated cycles of depolarisation and repolarisation, the nerve terminals generally maintained their responsiveness. However, with some nerve plates, these repeated cycles led to a gradual 'run down' in response

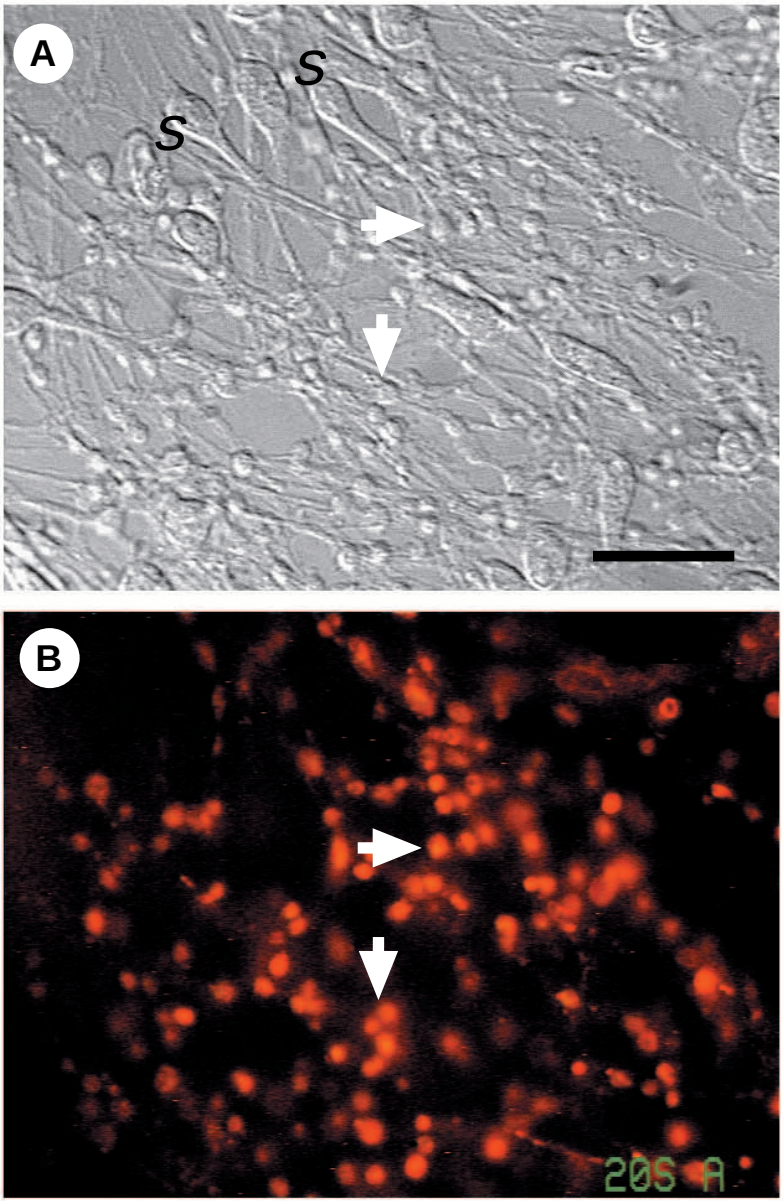

Fig. 4. Staining of nerve terminals with RH-414. Nerve plates from *Raja clavata* attached to a glass coverslip were transfered to the recording chamber of the optical imaging system and continuously perfused with skate Ringer. (A) Differential interference contrast image showing Schwann cells (*S*) and terminals (arrows). (B) Fluorescence image of the same preparation after being depolarised for 2 min with modified (K^+-containing) skate Ringer containing 5 μmol l^{-1} RH-414 and then washed for 5 min in skate Ringer. Following depolarisation, the dye was uniformly distributed throughout the nerve plate (not shown). All dye other than that entrapped in the synaptic vesicles of active nerve terminals (see Betz *et al.* 1992) was removed by the brief wash. Groups of nerve terminals clearly visible in both images are indicated by arrows. Scale bar (applies to A and B), 20 μm.

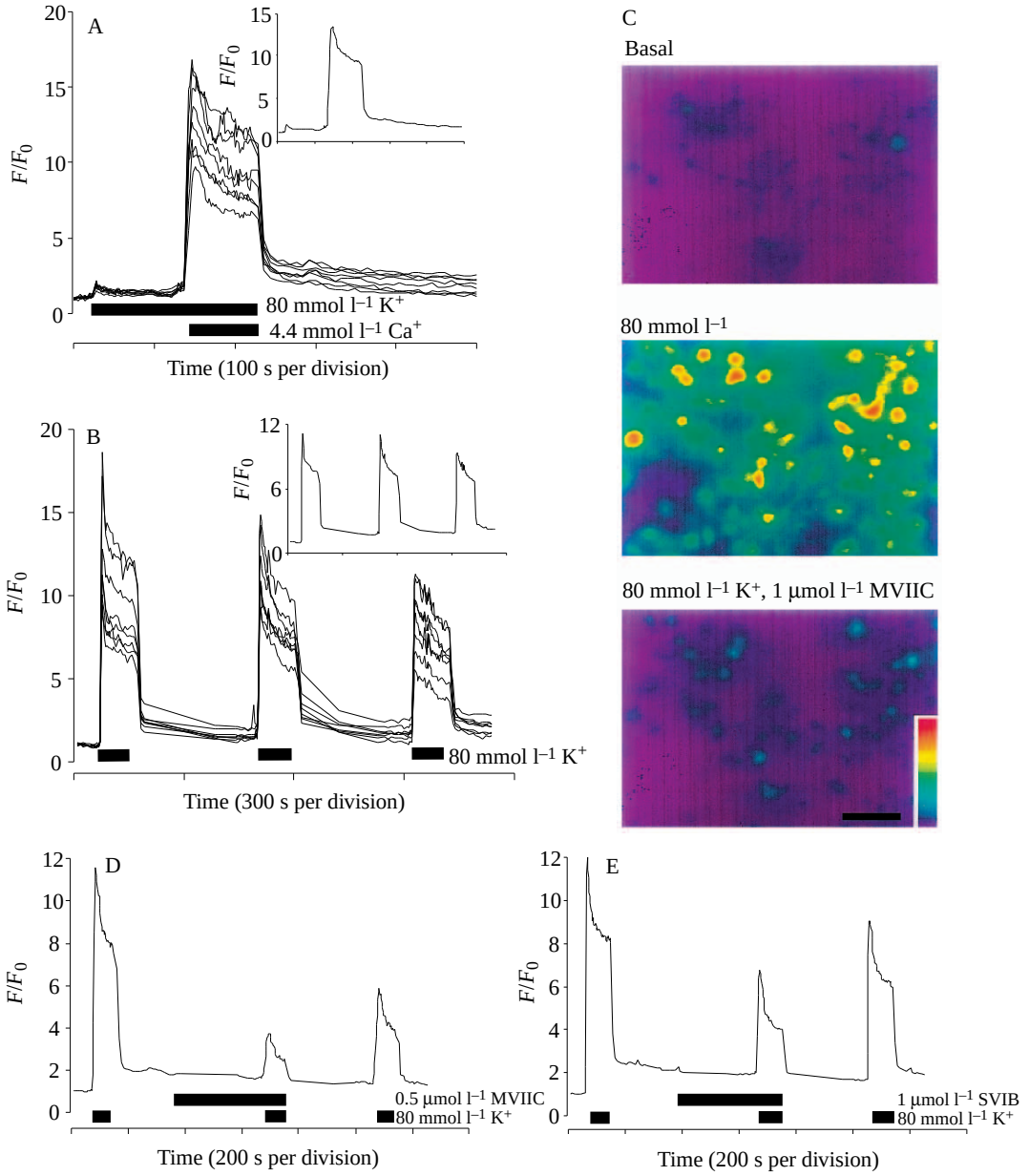

Fig. 5. Ca^{2+} responses in nerve terminals of depolarised nerve plates. *Raja brachyura* nerve plates loaded with Fluo-3 were placed in the perfusion/recording chamber and their fluorescence monitored as described in Materials and methods. All drugs and stimulations were applied *via* the perfusion medium (skate Ringer, SR). Changes or additions to the perfusion medium are indicated by the horizontal bars below the traces. The ordinate shows the ratio of the fluorescence intensity (F) to the initial baseline intensity (F_0) and is a measure of $[Ca^{2+}]_i$. (A) Ca^{2+} entry from the extracellular medium is necessary for K^+-stimulated increases of $[Ca^{2+}]_i$ in nerve terminals. Depolarisation in the absence of extracellular Ca^{2+} results in no appreciable rise of intraterminal $[Ca^{2+}]_i$ until Ca^{2+} is added to the perfusion medium. The main traces are from individual regions of interest in the fluorescence images, each corresponding to an individual nerve terminal. The inset shows the averaged response from 24 nerve terminals. (B) Nerve terminals maintain their responsiveness to multiple K^+ stimulations. Note the small amount of 'run down' and the incremental rise in the baseline fluorescence that was often seen in these preparations. The inset shows the averaged response from 42 nerve terminals from the same experiment. (C) Pseudocolour fluorescence images of part of a Fluo-3-loaded nerve plate preparation before K^+ stimulation and during stimulation in the absence and presence of 1 µmol l^{-1} ω-conotoxin MVIIC (MVIIC). Fluorescence intensity is calibrated according to the colour scale, which represents a linear scale of fluorescence intensity from 0 (violet) to 255 (red) arbitrary units. Under basal conditions, fluorescence output is very low; however, upon stimulation, nerve terminals appear as numerous punctate fluorescent dots over the upper surface of the nerve plate. This response is antagonised by 1 µmol l^{-1} ω-conotoxin MVIIC. Scale bar, 10 µm. (D,E) Two members of the ω-conotoxin family of voltage-sensitive Ca^{2+} channel antagonists, ω-conotoxin MVIIC (MVIIC; 0.5 µmol l^{-1}) and ω-conotoxin SVIB (SVIB; 1 µmol l^{-1}), antagonise the K^+-stimulated Ca^{2+} response in skate nerve terminals. Antagonists were added as indicated by the horizontal bars. Note that both the peak and plateau phases of the response are inhibited and that, in each case, the antagonism is at least partially reversible. The traces represent the average responses from 35 (D) and 57 (E) nerve terminals.

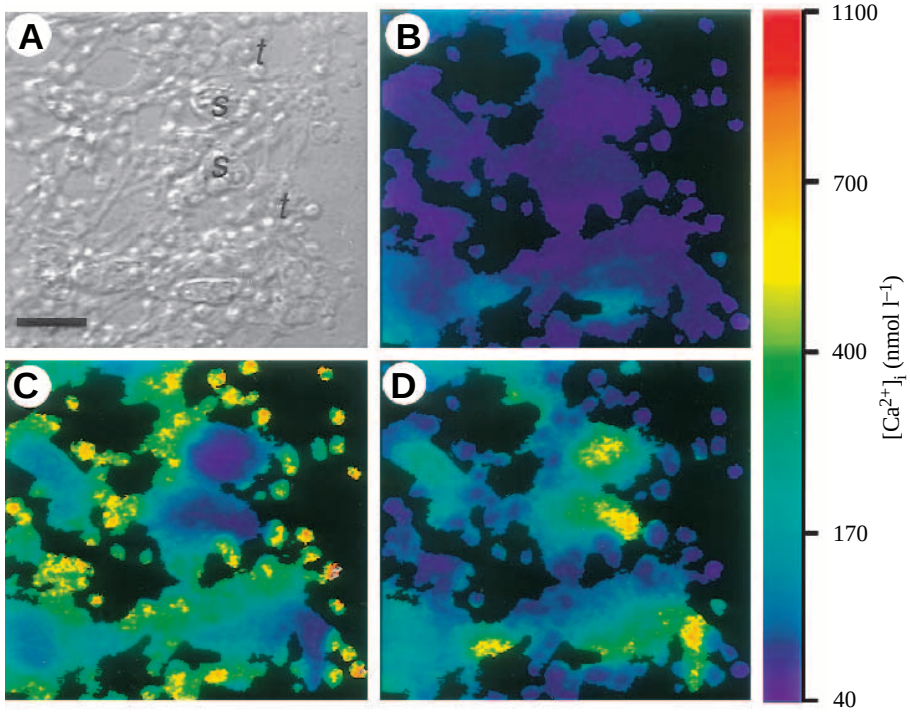

Fig. 6. Ca^{2+} responses in skate electric organ nerve plates. Nerve plates from *Raja brachyura* loaded with Fura-2 were monitored as described in Materials and methods. Fluorescence images were ratioed and analysed using IonVision software and the calibrated ratio images are shown in a pseudocolour display. (A) Both Schwann cells (*s*) and nerve terminals (*t*) can be seen clearly when using differential interference contrast optics. Scale bar, 10 μm. (B) Resting levels of $[Ca^{2+}]_i$ are generally below 100 nmol l^{-1} in both nerve terminals and Schwann cells in the nerve plate. (C) Stimulation with 80 mmol l^{-1} K^+ results in a marked increase of intraterminal $[Ca^{2+}]_i$ whereas Schwann cell $[Ca^{2+}]_i$ remains relatively low. (D) In contrast, when stimulated with ATP (50 μmol l^{-1}), Schwann cell $[Ca^{2+}]_i$ increases dramatically whilst intraterminal $[Ca^{2+}]_i$ remains unchanged. A 'halo' effect can be seen around certain nerve terminals and may represent the fine Schwann cell processes that can be seen in contact with the nerve terminals in transmission electron micrographs (see Fig. 3).

amplitude and incremental rises in baseline Ca^{2+} concentrations (Fig. 5B). It is likely, therefore, that the preparation of nerve plates occasionally results in some insult to the nerve terminals. When loaded with Fura-2, the brighter fluorescence from the Schwann cells often masked that from the smaller nerve terminals. However, Fluo-3 nerve terminal fluorescence was not masked by the Schwann cell signal. The Schwann cells loaded poorly with Fluo-3 as was indicated by the inability routinely to measure ATP-induced increases of Fluo-3 fluorescence in these cells (see below). Additionally, since the Schwann cells did not usually respond to depolarisation (see below) and the fluorescence output of Fluo-3 at resting $[Ca^{2+}]_i$ was very low, increases in nerve terminal Fluo-3 fluorescence were easily detected above the background (Fig. 5C). Thus, Fluo-3 was a more reliable indicator of changes in intraterminal $[Ca^{2+}]_i$.

Inhibition of the K^+-stimulated Ca^{2+} response in nerve terminals

Certain members of the ω-conotoxin family of Ca^{2+} channel antagonists (Olivera *et al.* 1994) have been used extensively to characterise voltage-sensitive Ca^{2+} channels. Two of these peptide antagonists, ω-conotoxin MVIIC and ω-conotoxin SVIB, inhibited the K^+-stimulated nerve terminal Ca^{2+} response in a concentration-dependent and reversible manner (Fig. 5C,D,E; Table 1; see also Richardson *et al.* 1995). Other peptide Ca^{2+} channel antagonists with analogous structure to the above ω-conotoxins failed to inhibit the Ca^{2+} response (Table 1). Likewise, nifedipine, at a concentration (5 μmol l^{-1}) selective for L-type channels, was also ineffective. However, at a higher, non-selective concentration (100 μmol l^{-1}), significant inhibition of the nerve terminal Ca^{2+} response was seen (Table 1).

Schwann cell Ca^{2+} responses

The Schwann cells in Fura-2-loaded nerve plates were also examined for their responsiveness to depolarisation. As can be

Table 1. *Antagonism of voltage-sensitive Ca^{2+} channels in skate electric organ nerve terminals*

Antagonist	Concentration (μmol l^{-1})	Percentage antagonism		*N*	
MVIIC	0.2		(37±8)		(4)
MVIIC	0.5	73±8	(68±6)	4	(3)
MVIIC	1	90±5	(76±2)	2	(7)
SVIB	1	59±3	(46±6)	5	(3)
SVIB	5	72±9		3	
MVIIA	1	7±2		4	
AgaIVA	0.3	7±3		2	
GVIA	5	7±3		2	
GVIA/AgaIVA	1/0.3	6±5		3	
Nifedipine	5	12		1	
Nifedipine	100	42±17		3	

Nerve plates from *Raja brachyura* and *R. montagui* were loaded with the Ca^{2+}-sensitive dyes Fluo-3 or Fura-2 and changes in $[Ca^{2+}]_i$ were monitored as described in Materials and methods. To normalise the data from different nerve plates, antagonists at the concentrations indicated were applied during the plateau phase of the K^+-stimulated Ca^{2+} response. The percentage inhibition of the plateau phase relative to the pre-stimulation baseline is given. Values are mean ± S.D. ($N \geq 3$) or mean ± range ($N=2$).

In each experiment, responses from between 20 and 55 nerve terminals were averaged.

Data from Fura-2-loaded nerve plates are given in parentheses.

MVIIC, ω-conotoxin MVIIC; MVIIA, ω-conotoxin MVIIA; GVIA, ω-conotoxin GVIA; SVIB, ω-conotoxin SVIB; AgaIVA, ω-agatoxin IVA.

seen in Fig. 6, Schwann cell $[Ca^{2+}]_i$ was essentially unresponsive to depolarisation. The small increase in $[Ca^{2+}]_i$ has the same time course as seen in the terminals and is most probably accounted for as a 'spill over' signal from responsive terminals lying in the Schwann cell fields but out of the plane of focus. In contrast to these weak responses, much larger responses to depolarisation were very occasionally seen in one or more of the Schwann cells in the field of view (in approximately one cell in 20). These responses were of comparable magnitude to those seen in nerve terminals but occurred 5–10 s after depolarisation and consisted of a monophasic rise and fall to baseline levels lasting in total for approximately 30 s even during sustained depolarisation. It seemed possible that these delayed responses could be secondary to transmitter release from the nerve terminals, with the probability of their observation being dependent on nerve terminals and Schwann cells being in a favourable orientation or in very close juxtaposition.

These observations prompted us to test for responses using exogenously applied transmitter and cotransmitter molecules. Since, in cholinergic nerve terminals, ATP is co-packaged with acetylcholine (ACh) in the synaptic vesicles (Dowdall *et al.* 1974), we tested the effect of applying these molecules to nerve plates. Schwann cells normally maintained a low resting $[Ca^{2+}]_i$ for periods of observation of up to 3 h (40±22 nmol l^{-1} mean ± S.D., N=232 cells; see Fig. 6). As can be seen in Fig. 7, ACh induced small (peak $[Ca^{2+}]_i$ 93±43 nmol l^{-1}, mean ± S.D.), delayed increases of $[Ca^{2+}]_i$ in some cells (16/36 cells). Although these responses appeared to be sensitive to atropine (5 μmol l^{-1}), suggesting the presence of muscarinic ACh receptors, their small and occasional nature prevented a detailed pharmacological characterisation. However, all the Schwann cells tested responded to application of ATP (50 μmol l^{-1}) with peak $[Ca^{2+}]_i$ reaching 320±121 nmol l^{-1} (mean ± S.D. from 146 cells) (Figs 6, 7). Multiple applications of ATP (50 μmol l^{-1}) elicited responses that showed little sign of run down (results not shown). As shown in Fig. 7, this response was concentration-dependent and was seen in the 1–100 μmol l^{-1} range. No response was seen in the nerve terminals during applications of ATP at 50 μmol l^{-1} (Fig. 6). A more complete description of the pharmacological features of this Schwann cell response will be provided elsewhere. Thus, the Schwann cells in the nerve plate preparation, like the nerve terminals, are viable and are capable of functional responses.

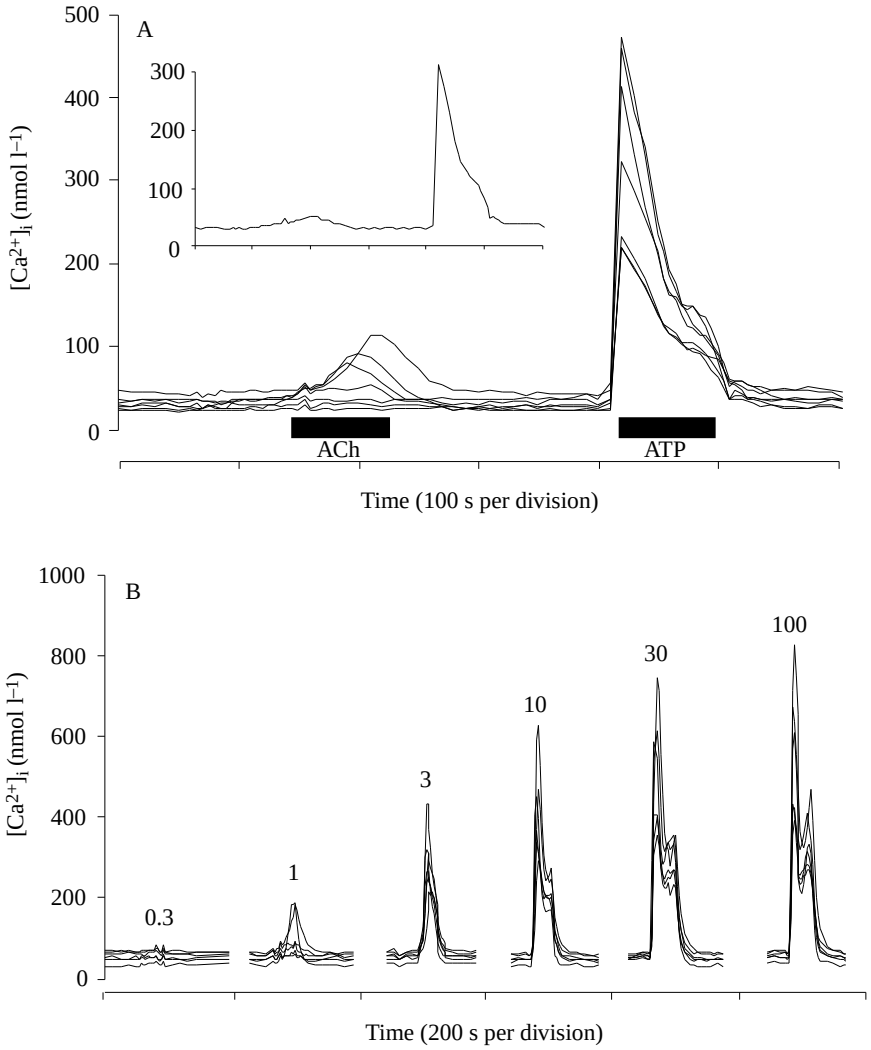

Fig. 7. Schwann cell Ca^{2+} responses to exogenously applied transmitters. (A) Nerve plates from *Raja brachyura* loaded with Fura-2 were continuously perfused with skate Ringer (SR) to which acetylcholine (ACh, 250 μmol l^{-1}) or ATP (50 μmol l^{-1}) was added as indicated by the horizontal bars below the main traces. ACh causes a modest and gradual increase of Schwann cell $[Ca^{2+}]_i$ in a proportion of the cells tested; in contrast, ATP induced a marked and rapid increase of $[Ca^{2+}]_i$ in all the cells examined. The inset shows the averaged response from all the cells in this experiment (N=7). (B) Nerve plates from *R. montagui* loaded with Fura-2 were continuously perfused with SR to which ATP at the indicated concentrations (in μmol l^{-1}) was added. Note the concentration-dependent increase of the Schwann cell Ca^{2+} response and the appearance of a biphasic peak and plateau phase at the higher concentrations.

Nerve plates from different species

The three species of skate used in this study all proved to be suitable sources of nerve plates with functional nerve terminals and Schwann cells. Nerve plates from *R. montagui* and *R. brachyura* were particularly good for dynamic imaging studies. Although they often formed a relatively thick cellular layer on glass coverslips, they possessed many functional nerve terminals and showed minimal 'run down' with repeated stimulation. In contrast, nerve plates from *R. clavata* formed a thinner cellular layer with fewer nerve terminals. Although this improved the identification of these structures (see Fig. 4), *R. clavata* preparations were prone to 'run down'.

Discussion

The first cytological descriptions of the cellular plexus innervating electrocytes in the skate electric organ date back to the last century (Ewart, 1888, 1892; Robin, 1865; Sanderson and Gotch, 1888, 1889). In Sanderson and Gotch (1888) can be found a translation of Robin's (1865) very lucid description of the arrangement and appearance of the nerve terminals in this plexus: 'On arriving at the surface of the disk (*sic* electrocyte) each fibre terminates in a pyramidal or conical body from four to five thousandths of a millimetre in length, the base of which is applied to the disk. The plexus of nerve with its terminations separates very easily from the disk and presents in surface view a finely granulated appearance with minute perforations here and there, the granules representing the terminal pyramids. On focussing below the surface, the field appears to be beset with minute points, which are the optical sections of the terminal fibres'. In the present paper, we describe a technique for isolating this plexus as an intact structure containing functional nerve terminals and supporting Schwann cells. This technique is based on the dissociating effect of collagenase previously described by Fox *et al.* (1990) and Kriebel *et al.* (1996). In these earlier studies, these structures were noted (see 'nerve ending clusters' in Kriebel *et al.* 1996) but were not examined in any detail.

When either detached from, or attached to, their electrocytes, nerve plates from collagenase-dissociated skate electric organ are extremely 'sticky' and adhere non-specifically to a variety of plastic or glass surfaces. This 'stickiness' has frustrated attempts to purify large numbers of nerve plates using sedimentation techniques (C. M. Richardson and M. J. Dowdall, unpublished observations). However, we have exploited this property to devise a simple technique that produces small numbers of nerve plates adhering to glass coverslips.

Structural examination of nerve plate preparations using light and electron microscopy has shown that they consist of a dense cellular matrix in which there are large clusters and strings of nerve terminals attached to branching nerve fibrils. Embedded in this matrix are Schwann cells with membrane processes which envelop the nerve fibrils and partially surround the nerve terminals. Previous cytological studies of this presynaptic plexus *in situ* (for examples, see Fox *et al.* 1990) reveal essentially the same cellular features as described above, and it therefore seems that the plexus survives the enzyme treatment and can be recovered as an intact and complete structure. It is also probable that our method for mechanically separating individual electrocytes from nerve plates leads to some loss of nerve terminals – those that may remain attached, by synaptic contact, to the electrocyte. Despite this unquantified loss, large numbers of nerve terminals remain associated with the nerve plate.

It seems likely that these nerve terminals are fully competent transmitter release sites, but a direct demonstration of this has not been possible in the present study because of the limited amounts of material available. The evidence for this is therefore indirect. Depolarisation-dependent rises in intraterminal $[Ca^{2+}]$, which were sensitive to two different ω-conotoxins, were consistently observed in all preparations of nerve plates. These observations strongly suggest the presence of resting potentials and operational voltage-sensitive Ca^{2+} channels. The two particular ω-conotoxins which block this response are also known to inhibit transmitter release in slices of electric organ depolarised with the same high-$[K^+]$ skate Ringer as used in the present experiments (Richardson *et al.* 1995, 1996). Additionally, Ca^{2+} channel antagonists without effect on transmitter release were also ineffective at inhibiting the K^+-stimulated Ca^{2+} response in nerve terminals. Thus, these results support our view that the presynaptic Ca^{2+} channel controlling transmitter release in skate electric organ has a pharmacology that is distinct from that at other peripheral and central synapses in its insensitivity to ω-conotoxin GVIA and ω-agatoxin IVA (Richardson *et al.* 1995, 1996).

That increases in intraterminal Ca^{2+} concentration resulted in transmitter release can be inferred from experiments in which the dye RH-414 became incorporated into the terminals as a consequence of depolarisation. This incorporation, which only occurs in terminals undergoing the membrane recycling associated with transmitter release (Betz *et al.* 1992), was also sensitive to ω-conotoxin MVIIC. These two sets of observations can leave little doubt that the nerve terminals in the nerve plate preparation are fully functional. A final strand of evidence for transmitter release is provided by the delayed response seen occasionally in Schwann cells of K^+-depolarised nerve plates. It is possible that this response is triggered by ATP released from the nerve terminals. Thus, capriciously, the arrangement of nerve terminals and Schwann cells in nerve plates may sometimes be favourable for 'internal' detection of the release of a chemical mediator from nerve terminals. These conclusions concerning the functional state of nerve terminals in nerve plates are fully concordant with previous electrophysiological observations on transmitter release by nerve terminals of innervated electrocytes isolated from collagenase-dissociated electric organ (Kriebel *et al.* 1996). In these preparations, spontaneous release, detected as miniature end plate potentials, was still detectable after 4 days of collagenase treatment at 6 °C and only ceased when collagenase denervation was complete (>6–7 days of collagenase treatment).

Prior to the present study, the Schwann cells of the innervation plexus of skate electrocytes have received little attention as interest has been focused on the nerve terminals. However, because the terminals are in intimate contact with Schwann cell processes (Fox *et al.* 1990), the emphasis in previous studies has been on devising methods to isolate nerve terminals freed from their encapsulating Schwann cell processes (Dowdall *et al.* 1989;

Kriebel *et al.* 1996). Schwann cells are integral components of nerve plates, and our studies on nerve terminals have therefore automatically included them. This has fortuitously revealed that these too are functionally competent in that they are able to respond to external chemical stimuli. Like glial cells elsewhere (Kastritsis *et al.* 1992; Salter and Hicks 1994), those in the nerve plate plexus give positive Ca^{2+} responses when stimulated with ATP. Recently, perisynaptic Schwann cells at the frog neuromuscular junction have been identified as a target for the synaptically released transmitters ACh and ATP (Jahromi *et al.* 1992; Reist and Smith, 1992; Robitaille, 1995). Both electrical stimulation of the nerve and exogenously applied transmitters stimulate an increase of $[Ca^{2+}]_i$ in these cells. Our finding, that skate electric organ perisynaptic Schwann cells also respond to ATP stimulation with an increase of $[Ca^{2+}]_i$, suggests that this response may be of general significance to transcellular signalling mechanisms at the cholinergic synapse.

The nerve plate preparation described in this paper has a number of features which make it an attractive model for studying synaptic mechanisms. These preparations with functional cellular components are simple to obtain from the electric organs of all skate species so far tested. The physiological robustness of excised electric organs and the large number of nerve plates found in each organ (e.g. 2.5×10^3 in *R. clavata*) offer the possibility of numerous experiments from the material available from a single fish. So far, functional studies using nerve plates have been limited to investigations using imaging technology. However, other techniques deserve consideration and might also be equally successful. The size and accessibility of the Schwann cells and the large (up to 5 μm in diameter) nerve terminals in the nerve plates make them good candidates for electrophysiological studies using patch electrodes. If successful, this approach might greatly facilitate investigations on the functional interactions between nerve terminals and Schwann cells indicated by the present study. Biochemical studies with nerve plates would require more material than can be conveniently prepared by the technique described in this paper, and these must therefore await the development of a bulk isolation method of high yield.

C.M.R. was supported by a CASE studentship from the BBSRC with Lilly Research Laboratories. Fluorescence imaging equipment was funded by the University of Nottingham and the Wellcome Trust (043043/Z/94/Z). We thank Mr T. Smith for valuable technical assistance with electron microscopy.

References

BENNETT, M. V. L. (1961). Modes of operation of electric organs. *Annls N.Y. Acad. Sci*. **94**, 458–509.

BENNETT, M. V. L. (1970). Electric organs. *A. Rev. Physiol.* **32**, 471–528.

BETZ, W. J., MAO, F. AND BEWICK, G. S. (1992). Activity-dependent fluorescent staining and destaining of living vertebrate motor nerve terminals. *J. Neurosci.* **12**, 363–375.

BROCK, L. G., ECCLES, R. M. AND KEYNES, R. D. (1953). The discharge of individual electroplates in *Raia clavata*. *J. Physiol., Lond.* **122**, 4P–6P.

COUTEAUX, R. (1963). The differentiation of synaptic areas. *Proc. R. Soc. B* **158**, 457–480.

DOWDALL, M., PAPPAS, G. AND KRIEBEL, M. (1989). Properties of detached nerve terminals from skate electric organ: a combined biochemical, morphological and physiological study. *Biol. Bull.* **177**, 322.

DOWDALL, M. J., BOYNE, A. F. AND WHITTAKER, V. P. (1974). ATP: A constituent of cholinergic synaptic vesicles. *Biochem. J.* **140**, 1–12.

DOWDALL, M. J. AND ZIMMERMANN, H. (1977). The isolation of pure cholinergic nerve terminal sacs (t-sacs) from the electric organ of juvenile *Torpedo*. *Neuroscience* **2**, 405–421.

EWART, J. C. (1888). The electric organ of the skate. *Phil. Trans. R. Soc.* **179**, 399–416.

EWART, J. C. (1892). The electric organ of the skate – observations on the structure, relations, progressive development and growth of the electric organ of the skate. *Phil. Trans. R. Soc.* **183**, 389–420.

FOX, G. Q., KRIEBEL, M. E. AND PAPPAS, G. D. (1990). Morphological, physiological and biochemical observations on skate electric organ. *Anat. Embryol.* **181**, 305–315.

JAHROMI, B. S., ROBITAILLE, R. AND CHARLTON, M. P. (1992). Transmitter release increases intracellular calcium in perisynaptic Schwann cells *in situ*. *Neuron* **8**, 1069–1077.

KARNOVSKY, M. J. AND ROOTS, L. (1964). A 'direct-coloring' thiocholine method for cholinesterases. *J. Histochem. Cytochem.* **12**, 219–221.

KASTRITSIS, C. H. C., SALM, A. K. AND MCCARTHY, K. (1992). Stimulation of the P_{2Y} purinergic receptor on type 1 astroglia results in inositol phosphate formation and calcium mobilisation. *J. Neurochem.* **58**, 1277–1284.

KRIEBEL, M. E., DOWDALL, M. J., PAPPAS, G. D. AND DOWNIE, D. (1996). Detached, purified nerve terminals from skate electric organ for biochemical and physiological studies. *Biol. Bull.* **190**, 88–97.

OLIVERA, B. M., MILJANICH, G. P., RAMACHANDRAN, J. AND ADAMS, M. E. (1994). Calcium channel diversity and neurotransmitter release: the ω-conotoxins and ω-agatoxins. *A. Rev. Biochem.* **63**, 823–867.

REIST, N. E. AND SMITH, S. J. (1992). Neurally evoked calcium transients in terminal Schwann cells at the neuromuscular junction. *Proc. natn. Acad. Sci. U.S.A.* **89**, 7625–7629.

RICHARDSON, C. M., DOWDALL, M. J. AND BOWMAN, D. (1996). Inhibition of acetylcholine release from presynaptic terminals of skate electric organ by calcium channel antagonists: a detailed pharmacological study. *Neuropharmac.* **35**, 1537–1546.

RICHARDSON, C. M., DOWDALL, M. J., GREEN, A. C. AND BOWMAN, D. (1995). Novel pharmacological sensitivity of the presynaptic calcium channels controlling acetylcholine release in skate electric organ. *J. Neurochem.* **64**, 944–947.

ROBIN, M. C. (1865). Memoire sur la démonstration expérimental de la production d'électricité par un appareil propre aux poissons du genre des *Raies*. *J. Anat. Physiol.* **2**, 507–535.

ROBITAILLE, R. (1995). Purinergic receptors and their activation by endogenous purines at perisynaptic glial cells of the frog neuromuscular junction. *J. Neurosci.* **15**, 7121–7131.

SALTER, M. AND HICKS, J. L. (1994). ATP-evoked increases in intracellular calcium in neurones and glia in the dorsal spinal cord. *J. Neurosci.* **14**, 1563–1575.

SANDERSON, J. B. AND GOTCH, F. (1888). On the electric organ of the skate. *J. Physiol., Lond.* **9**, 137–166.

SANDERSON, J. B. AND GOTCH, F. (1889). On the electrical organ of the skate. Part II. *J. Physiol., Lond.* **10**, 259–278.